

# Study the Properties of Cu-Zn Ferrite Substituted with Rare Earth Ions by Using Positron Annihilation Analysis

A.M. Samy\*, E. Gomaa and N. Mostafa

Physics Department Faculty of Science, Ain Shams University, Abbassia – 11566, Cairo, Egypt

**Abstract:** Positron annihilation lifetime spectroscopy (PALS) is a direct probe of size and concentration of nano-scale defects in materials, because it is very sensitive to electron density. The lifetime of positron ( $\tau$ ) and its intensity ( $I$ ) can be used to characterize the defects concentration. In the present work, PALS has been applied to measure the variation of positron lifetime parameters for polycrystalline samples with chemical formula  $Zn_{0.5}Cu_{0.5}Fe_{1.98}R_{0.02}O_4$  ( $R = Gd, Sm, Nd$  and  $La$ ). The variation of positron annihilation lifetime parameters ( $I_1, I_2, \tau_{av}$  and  $k$ ) with the ionic radius of rare earth ions, homogeneity, grain size and electrical resistivity have been studied. The inter-granular pores and grain boundaries defects are increased with the increasing of the ionic radius of the rare earth ions and decreased for Gd-sample. The defects inside and outside the grains are distributed homogeneously for Sm-sample only. A positive correlation has been found between positron lifetime parameters and ionic radius of rare earth ions as well as the electrical resistivity.

**Keywords:** Ferrites, rare earth ions, positron annihilation, resistivity.

## 1. INTRODUCTION

Ferrites have very important applications according to their electrical and magnetical properties. The substitution effect and the change of the preparation condition are allowed to improve some ferrites with different composition to be used in wide frequency range, from microwaves to radio wave frequencies. A considerable amount of work has been carried out on Cu–Zn ferrite substituted with rare earth ions of different kind and concentration [1-3]. It was found that, the initial permeability and the homogeneity of the composition  $Zn_{0.5}Cu_{0.5}Fe_{1.98}R_{0.02}O_4$  were increased for the samples with  $R = Nd, Sm$  and  $Gd$  while the resistivity was increased for the samples with  $R = La$  and  $Nd$  relative to the unsubstituted one,  $R = none$ . The improvement of the resistivity was attributed to the decrease of grain size and the increase of the porosity of the samples. From this point of view, we aimed in this paper to investigate the microstructure and the defects on the atomic scale of the composition  $Zn_{0.5}Cu_{0.5}Fe_{1.98}R_{0.02}O_4$  ( $R = Gd, Sm, Nd$  and  $La$ ) by using the positron annihilation lifetime spectroscopy (PALS) analysis. (PALS) is a valuable nuclear method to investigate the materials without damage them [4, 5]. PALS has a high sensitivity for probing vacancy defects through measurements of positron lifetime. It is based on the high sensitivity of positron to localize at low electrons density regions of a material and the emission of annihilation gamma rays that escape from the system without any interaction. These gamma rays hold information about the defects around the annihilation site.

A correlation is established between the positron lifetime parameters and the ionic radius of the rare earth ions, grain size as well as the electric resistivity. The PALS is a good

tool to analyze the defects inside and outside the grains of the ferrite samples. From our view, it is a very interesting new technique to analyze ferrite samples which may help to understand different properties of ferrites. In future, PALS could be used to investigate different compositions of ferrites by different researchers.

## 2. EXPERIMENTAL TECHNIQUES

Polycrystalline samples with chemical formula  $Zn_{0.5}Cu_{0.5}Fe_{1.98}R_{0.02}O_4$  ( $R = Gd, Sm, Nd$  and  $La$ ) are prepared by solid - solid reaction method (ceramic method). The oxides  $Fe_2O_3, CuO, ZnO$  and  $R_2O_3$  with purity 99.99% are weighted in stoichiometric proportions. All oxides of each sample are mixed together and ground to very fine powder. These powders are presintered at 900 °C for 30 hr then slowly cooled. The mixture of each sample is ground again, pressed into disc form and final sintered at 1000 °C for 6 hr and then slowly cooled to the room temperature. Using a diffractometer type (X'Pert Graphics), X-ray diffraction patterns are performed to confirm the formation of a single cubic spinel phase for all samples. The lattice parameter was calculated from the following relation:  $a = d_{hkl} (h^2 + k^2 + l^2)^{1/2}$ , where  $h, k$  and  $l$  are the Miller indices of each peak and  $d_{hkl}$  is the d-spacing. The porosity percentage is calculated according to the relation [6]:  $P = 100[1 - d/d_x] \%$ , where  $d_x$  is the X-ray density and is calculated using the following formula:  $d_x = 8M / Na^3$  where  $M$  is the molecular weight of each sample,  $N$  is Avogadro's number and  $a$  is the calculated average lattice parameter. The density of the sample,  $d$  ( $g/cm^3$ ) is measured in toluene using Archimede's principle. It is calculated according to the following formula:

$$d = [m_s / (m_s - m_t)](d_t),$$

where  $m_s$  is the mass of the sample in air,  $m_t$  is the mass of the sample in toluene and  $d_t$  is the density of toluene. The scanning electron microscope type JEM – 1200 EXII is used to observe the microstructure for all samples. All samples are polished and etched before taking the micrographs. The

\*Address correspondence to this author at the Physics Department Faculty of Science, Ain Shams University, Abbassia – 11566, Cairo, Egypt; Tel/Fax: +(202) 682-2189; E-mail: amanisami6@hotmail.com

average grain size (G.S) was obtained by counting the number of the grain boundaries intercepted by measured lengths of random straight lines drawn on the micrographs of these samples. The homogeneity of the samples is calculated from the initial permeability curves against the temperature. Further details are recommended in ref. [2].

Positron annihilation lifetime spectra are measured using a fast-fast coincidence system at room temperature. The time resolution of 230 ps for  $^{60}\text{Co}$  and each spectrum contained more than 1 million counts. 20  $\mu\text{Ci}^{22}\text{Na}$  source is deposited on a thin Kapton foil (7  $\mu\text{m}$ ) and sandwiched between two similar samples. The obtained lifetime spectra are processed by PATFIT program [7]. The spectra are decomposed into two components, so that the two lifetime components  $\tau_1$  and  $\tau_2$  which was corresponding to  $I_1$  and  $I_2$  are extracted. The component characterized by  $\tau_1$  and  $I_1$  represents positrons annihilation in the matrix and dislocation loops. The component  $\tau_2$  and  $I_2$  characterizes the trapping and annihilated of positrons in three dimensional mono-vacancies and vacancy clusters defects. The average lifetime  $\tau_{av}$ , which reflects the overall performance of materials under the positron environment, is calculated by using the following formula:

$$\tau_{av} = \tau_1 I_1 + \tau_2 I_2.$$

The trapping rate ( $\kappa$ ) which represents the ability of defect to capture positrons is calculated according to the two-state trapping model [8] by the following formula :  $\kappa = I_2 / I_1(1/\tau_1 - 1/\tau_2)$ .

### 3. RESULTS AND DISCUSSION

The variations of the average lifetime ( $\tau_{av}$ ), relative intensity ( $I_2$ ), and the trapping rate of the positrons ( $\kappa$ ) with the ionic radius of rare earth ions ( $r$ ) at the defect sites are shown in Fig. (1a, b). These figures illustrate the sensitivity of positron lifetime for the concentration of defects in our studied samples. As shown in the figures, the positron lifetime parameters  $\tau_{av}$ ,  $I_2$  and  $\kappa$ , at first are decreased with the increasing of the ionic radius of the rare earth ions for the sample with  $R = \text{Sm}$ , then they are increased for all the other samples. This means that, the large ionic radius of the rare earth ions permits the positron to reside at the defect sites with long lifetime ( $\tau_{av}$ ) and high concentration ( $I_2$ ). Thereby, the highest values of ( $I_2$ ) and ( $\kappa$ ) for the sample with  $R = \text{La}$  indicating that it has the highest defect concentration and trapping rate of the positron at the defect sites (Fig. 1b). For all samples, ( $I_2$ ) represents the sum of the defects due to the grain boundaries thicknesses and the inter-granular pores. The values of the ionic radius ( $r$ ) of rare earth ions and the grain size (G.S) for all samples are included in Table 1. It is clear that, there is an inversely relation between the ionic radius of the rare earth ions and the grain size of the samples. Meanwhile, the variation of  $\tau_{av}$ ,  $\kappa$  and  $I_2$  positron parameters with the grain size (G.S) are shown in Fig. (2a, b) for all samples. These parameters are decreased with the increasing of the grain size for all samples and then increased for the sample with  $R = \text{Gd}$ . As recommended by Dong *et al.* [5], when the grain size of the sample is increased the thickness of the grain boundaries is decreased. This indicating that, the size and the concentration ( $\tau_{av}$  and  $I_2$ ) of the nanoscale defects are due to the grain boundaries thickness as well as the number of positron trapped at these defects ( $\kappa$ ) are decreased

with increasing the grain size (G.S). Accordingly, the thickness of grain boundaries defect are increased with the increasing of the ionic radius of rare earth ions. Then, the increase of  $I_2$  with increasing the ionic radius of rare earth ions is attributed to the increase of grain boundaries defect. This leads to increase the positron annihilation parameters.

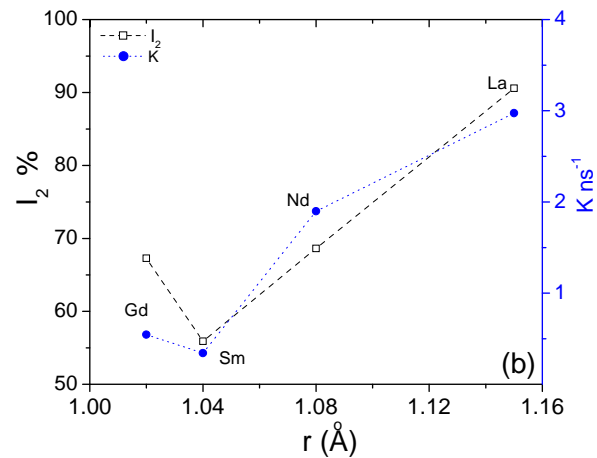
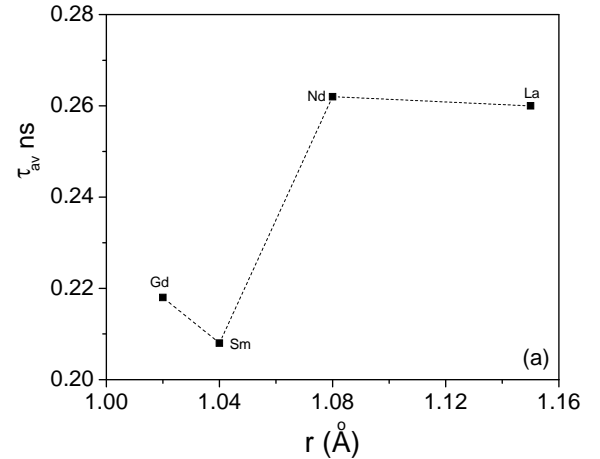


**Fig. (1).** (a) The variation of average lifetime ( $\tau_{av}$ ) with the ionic radius of rare earth ions ( $r$ ). (b) The variations of relative intensity ( $I_2$ ) and trapping rate of positrons ( $\kappa$ ) with the ionic radius of rare earth ions ( $r$ ).

On the other hand, it is known that for the samples that prepared by ceramic method, the total porosity result from the sum of inter-granular porosity, ( $P_{inter}$ ) and intra-granular porosity, ( $P_{intra}$ ),  $P$  (%) = ( $P_{inter} + P_{intra}$ ) [9]. Table 1 is revealed that, the total number of pores is increased with increasing the ionic radius ( $r$ ) of rare earth ions for all samples except the sample substituted with Sm ions. This may be attributed to the formation of  $\text{SmO}_2$  during the preparation condition [3]. Similar conclusion was reported for Ta - doped Mn - Zn ferrite [10].

Similar increase has been observed by our previous study on Mn - Zn ferrite substitutes with rare earth oxides [11]. Accordingly, the inter-granular pores may be increase with the increasing of the ionic radius of the rare earth ions. This can be conformed through the following discussion:

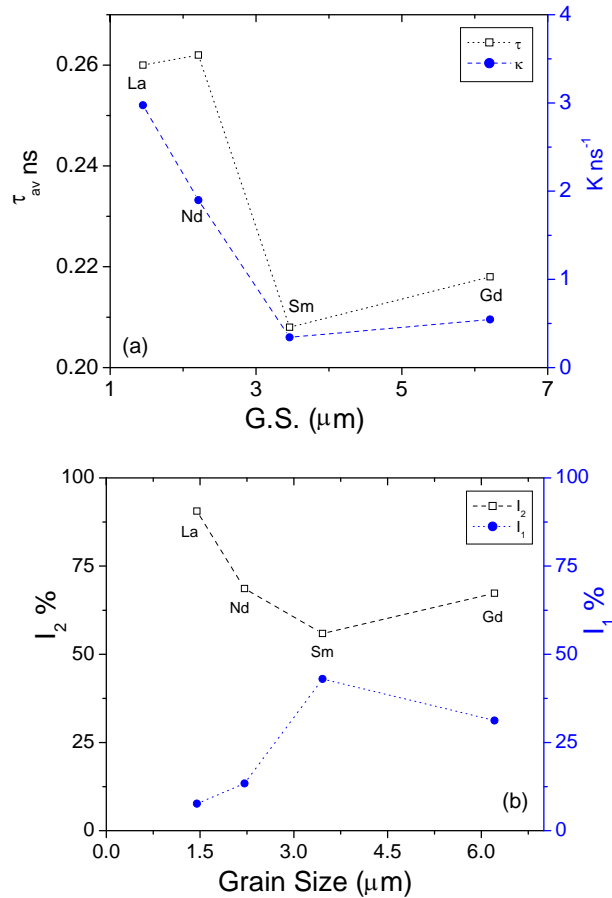


**Fig. (2).** (a) The variation of  $\tau_{av}$  and  $\kappa$  with the grain size (G.S) of the samples. (b) The variation of  $I_1$  and  $I_2$  with the grain size (G.S) of the samples.

**Table 1.** The Values of Ionic Radius (r), Porosity (P %) and Grain Size (G.S) for Cu-Zn Ferrites Substituted with Rare Earth Ions

R	r (Å)	Porosity (P %)	G.S. ( $\mu\text{m}$ ) $\pm 0.05 \mu\text{m}$
La	1.15	12.33	1.45
Nd	1.08	11.33	2.21
Sm	1.04	9.945	3.46
Gd	1.02	10.895	6.21

For all samples  $I_1$  is increased with the increasing of the (G.S) and then decrease for the sample with R = Gd as clear in Fig. (2b). This indicated that, the number of pores inside the grains (intra-granular pores),  $I_1$ , is increased with the increasing of the grain size for Cu-Zn ferrite substituted with La, Nd and Sm ions, then decreases for the sample substituted with Gd ions (Fig. 2b). One can concluded the decrease of inter – granular pores with the increasing of the G.S. for La, Nd and Sm samples and then increase for Gd – sample. This means that the decrease of  $I_2$  with the increasing of the G.S for all samples and then increase for the sample with R = Gd. The experimental results is conformed this conclusion (Fig. 2b). Consequently, the

number of inter – granular pores increases with the increasing of the ionic radius of the rare earth ions. This is because the ionic radius is inversely proportional with the grain size of the samples (Table 1). Accordingly, we can attribute the increase of  $I_2$  with the increasing of the ionic radius of rare earth ions to both the increase of grain boundaries defect and the number of inter- granular pores (Fig. 1b).

For the sample with R = Gd, the decrease of  $I_1$  with the increasing of the G.S. relative to all samples can be discussed as follows:

The Gd sample has large grain size compared with all the other samples which plays a role in decreasing the number of intra- granular pores,  $I_1$  (Table 1). This conclusion is conformed experimentally (Fig. 2b). Also, it was reported that the number of inter – granular porosity depends on the grain size [12]. The large increase of its grain size relative to all other samples leads to increase the number of inter-granular pores. Then, the number of the inter-granular pores may dominant the grain boundaries defects for Gd sample. This accounts on the increase of  $I_2$  for Gd sample (Fig. 2b). Accordingly, as the grain size is increased, G.S. > 3.46  $\mu\text{m}$ , the number of inter-granular pores as defects is increased and can dominant the grain boundaries thickness defects. This means that the dominant defect of  $I_2$  is the number of inter - granular pores for the Gd sample only. It is reported that the dominant defects of  $I_2$  was inter– granular pores for almost samples for Mn – Zn ferrite substituted with the rare earth ions,  $\text{Mn}_{0.6}\text{Zn}_{0.4}\text{Fe}_{1.9}\text{R}_{0.1}\text{O}_4$  (R = La, Nd, Sm, Gd and Dy) [11].

We can concluded that, PALP technique can be use to determine qualitatively the distribution number of pores inside and outside the grains. This plays an important role to study the physical, electrical and magnetical properties of ferrites.

The variation of  $I_1$  and  $I_2$  with the homogeneity,  $\Delta\mu_i/\Delta T$ , for all samples of Cu-Zn ferrites substituted with the rare earth ions are shown in Fig. (3). As can be seen from the figure, the sample substituted with Sm ions has the highest homogeneity value. This can be attributing to the nearly similar distribution of defects inside and outside the grains,  $I_1$  and  $I_2$  respectively. Accordingly, the highest homogeneity means the equally distribution of defect inside and outside the grains, do not mean the absence of defect because the samples are polycrystalline.

The variation of electric resistivity ( $\rho$ ) with  $\tau_{av}$  and  $\kappa$  for all studied samples are observed in Fig. (4). It is clear that  $\kappa$  is increased with the increasing of the electrical resistivity,  $\rho$ , for all studied samples. The increase of the electrical resistivity means the decrease of the hopping of the electrons at B-sites between  $\text{Fe}^{3+}$  and  $\text{Fe}^{2+}$  ions [12]. It was reported that  $\text{Fe}^{2+}$  ions are formed during the preparation condition due to oxygen loss [13]. IR is confirmed the presence of  $\text{Fe}^{2+}$  ions and the rare earth ions at B – sites [12]. This permits the positrons to have long average lifetime,  $\tau_{av}$  and large trapping rate. The figure also is revealed that, the average life time for the positron,  $\tau_{av}$ , is increased with the increasing of the resistivity except for the sample with R = La. This means that as the number of inter-granular pores is increased the positron can reside with longer lifetime at the defect

sites. The exception for La-sample may be attributed to the presence of La ions at the grain boundaries. Our conclusion agrees with that recommended by [1, 11, 14] for Cu-Zn ferrites and Li-Ni ferrites. This means that the positron annihilation is a good technique to study if there is any distribution for the cations at grain boundaries or all cations are distributed inside the grains of the ferrites.

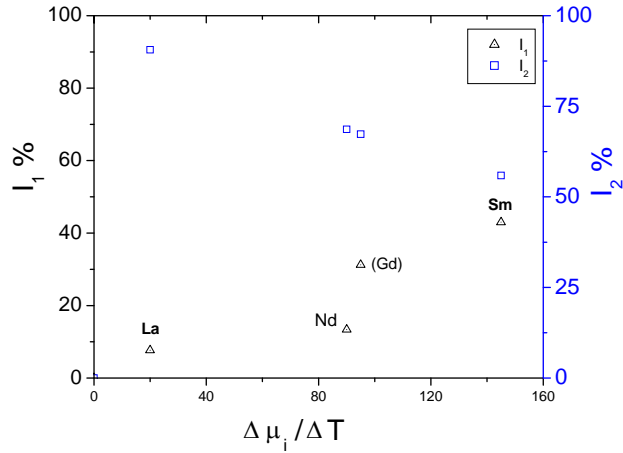


**Fig. (3).** The variation of  $I_1$  and  $I_2$  with the homogeneity,  $\Delta\mu_i/\Delta T$ , of the samples.

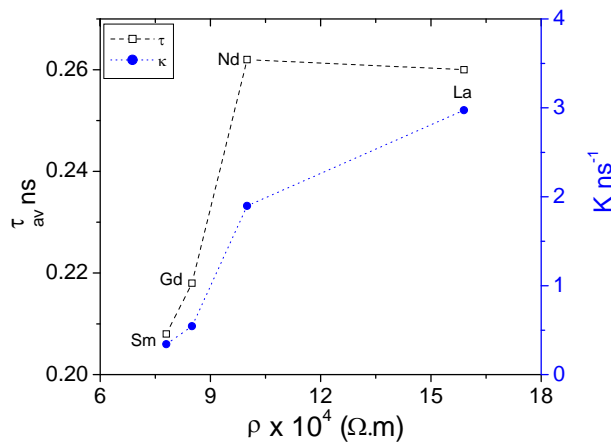


**Fig. (4).** The variation of  $\tau_{av}$  and  $\kappa$  with the electric resistivity ( $\rho$ ) of the samples.

#### 4. CONCLUSION

For  $Zn_{0.5}Cu_{0.5}Fe_{1.98}R_{0.02}O_4$  ( $R = Gd, Sm, Nd, La$ ), there is an inverse relation between the ionic radius of rare earth ions and grain size of the samples. The grain boundaries thickness, inter-granular pores (concentration of nanoscale defects) and trapping rate of positrons are increased with the

increasing of the ionic radius of rare earth ions except for Sm sample. The concentration of intra-granular pores increases with the increasing of the grain size of the samples, for  $G.S < 3.46 \mu m$  and decreases for  $G.S \geq 3.46 \mu m$ . For Sm sample, the defects are nearly equal in distribution inside and outside the grains, so it has the highest homogeneity. The average lifetime of positron increases with the increasing of the electrical resistivity for all samples and decreases for La sample. PALS will be a good technique to study if there is any distribution for cations at grain boundaries, or all cations distributed inside the grains in ferrites.

#### ACKNOWLEDGEMENTS

The authors would like to express their deepest thanks to Prof. Dr. M. Mohsen, head of Nuclear-Solid State Lab. and Prof. Dr A.A. Sattar, head of Magnetism Lab. Physics Dep. Faculty of Science, Ain Shams University.

#### REFERENCES

- [1] A. A. Sattar, A. H. Wafik, K. M. El-Shokrofy and M. M. El Tabby, "Magnetic properties of Cu-Zn Ferrites doped with rare earth oxides", *Phys. Stat. Sol.*, vol.171, pp. 563, 1999.
- [2] A. M. Samy, "Improvement of the magnetic and electrical properties of Cu-Zn ferrites", *J. Mater. Eng. Perform.*, vol. 12, p. 569, 2003.
- [3] A. A. Sattar and A. M. Samy, "Effect of Sm substitution on the magnetic and electrical properties of Cu-Zn ferrite", *J. Mater. Sci.*, vol. 37, p. 4499, 2002.
- [4] M. Eldrup and B. N. Singh, "Studies of defects and defect agglomerates by positron annihilation spectroscopy," *J. Nucl. Mater.*, vol. 251, p.132, 1997.
- [5] Y. Dong, L. Y. Xiong and C. W. Lung, "Positron annihilation at grain boundaries in Zn-22 wt% Al alloy," *J. Phys. Condens. Matter*, vol. 3, p. 3155, 1991.
- [6] K. J. Standely, *Oxide Magnetic Materials*, Clarendon Press: Oxford, 1972.
- [7] P. Kirkegaard, M. Eldrup, O. E. Mogensen and N. Pedersen, "Program system for analysing positron lifetime spectra and angular correlation curves," *Comput. Phys. Commun.*, vol. 23, p. 307, 1981.
- [8] P. Hautojarvi, *Positrons in Solid*, Springer: Berlin, 1979.
- [9] A. M. Samy, N. Mostafa and E. Gomaa, "Effect of rare earth substitutions on some physical properties of Mn-Zn ferrite studied by positron annihilation lifetime spectroscopy", *J. Appl. Surface Sci.*, vol. 252, p. 3323, 2006.
- [10] Y. Yamamoto, A. Makino and T. Nikaidou, "Electrical and magnetic properties of Ta-doped polycrystalline Mn-Zn ferrite", *J. Phys. IV.*, vol. 7, pp. C1 – 121, 1997.
- [11] W. D. Kigery, H. K. Bowen, D. R. Uhlmann, *Introduction of Ceramics*, John Wiley and Sons: London, 1975, p. 458.
- [12] N. Rezalescu, E. Rezlescu, C. Pasnicu and M. L. Craus, "Effect of the rare earth ions on some properties of a nickel-zinc ferrite", *J. Phys., Condens. Matter*, vol. 6, p. 5707, 1994.
- [13] S. Chikazumi and H. S. Charap, *Physics of Magnetism*, John Wiley and Sons, New John Wiley and Sons: New York, 1964, p. 153.
- [14] A. A. Sattar, A. H. Wafik and H. M. El-Sayed, "Transport Properties of trivalent substituted li-ferrites", *J. Mater. Sci.*, vol. 36, p. 4703, 2001.